SUPPLEMENTAL FILE - Cepeda-Garcia et al.

Actin-mediated delivery of astral microtubules instructs Kar9p asymmetric loading to the bud-ward spindle pole

Figure S1. Distribution of preanaphase cells according to their labeling by Kar9p-GFP_3 relative to both spindle alignment and SPB identity. Categories for preanaphase aligned spindles in which Kar9p label favored the SPB_{bud} were added and depicted in black in the simplified Figure 1 D. Categories for preanaphase aligned spindles in which Kar9p favored the SPB_{mother} were added and depicted in grey in Figure 1 D. The frequency of *preanaphase spindle misalignment* was 10.7% in wild type, 25% in *bud6*Δ, 40% in *bni1*Δ and 51.3% in *bud6*Δ *bni1*Δ cells; n > 390

Figure S2. (A-B) Disruption of Kar9p polarity occurs in response to both LatB and LatA and it is not mediated by the cell morphogenesis checkpoint. Cells were released from G_1 arrest and allowed to bud prior to the indicated treatments. Kar9p localization was then scored from digital images. (A) 200μM LatA promotes loss of Kar9p polarity as well as LatB. Wild type cells were treated for 15 min (n_{DMSO} = 165; n_{LatA} = 133; n_{LatB} = 179 short spindles) and 30 min (n_{DMSO} = 117; n_{LatA} = 278; n_{LatB} = 256 short spindles). (B) A *swe1*Δ mutation did not prevent loss of Kar9p polarity upon LatB treatment (n >153 short spindles). (C -D) Increase of Kar9p symmetry in response to LatB treatment is not prevented by a reduction in aMT dynamics (*tub2*^{C354S}). (C) Plot showing increased Kar9p symmetry upon LatB treatment in a *tub2*^{C354S} mutant, n > 100. (D) Representative images for Kar9p labeling following LatB treatment in a *tub2*^{C354S} mutant. Overlays of Kar9p-GFP_3 (green) and CFP-Tub1p (magenta) are shown. Bar, 2 μm. (E) LatB treatment increases Kar9p symmetry in a *mad2*Δ mutant. Cells were treated as in (A) and Kar9p recruitment scored from digital images; n > 117.

Figure S3. Actin integrity is required to establish and maintain Kar9p polarization to the SPB_{bud}. (A) Wild type cells were released from G_1 arrest into synthetic medium containing 0.1 M hydroxyurea. Samples were removed every 15 min to monitor budding and progression of the spindle pathway; n = 300 cells. The percentage of short spindles at the late treatment was the same for DMSO and LatB treated cells. Following bud emergence (black arrow) one sample of the synchronous culture was removed for early treatment. A second sample was taken after spindle assembly was complete (blue arrow) for late treatment. Each sample was split for incubation in 100 μM LatB or DMSO for 15 and 30 min. (B) Kar9p localization was scored following each treatment (early: n_{DMSO} > 71, n_{LatB} > 125 short spindles; late: n > 274 short spindles) from digital images. (C) Representative images corresponding to the 15-min late treatment with DMSO (top) or LatB (bottom) from the same experiment are shown. Notice that in the late treatment, Kar9p symmetric localization increased without disruption of spindle orientation. Overlays (left panel) of Kar9p-GFP_3 (green) and CFP-Tub1p (magenta) are shown. Bar, 2 μm.

Figure S4. Kar9p repolarization during recovery from nocodazole treatment in cell polarity mutants. (A-B) Time course following nocodazole washout was carried out as described in Figure 5. Kar9p localization was scored in digital images of the indicated strains (A) along with progression of the spindle pathway (B) following nocodazole washout. (C) Kar9p behavior during recovery from nocodazole treatment. Cells of the indicated strains were subject to recordings as described in Figure 6. Overlays of images for Kar9p (in green) and Spc42p (in magenta) are shown. In a wild type cell (top), Kar9p was initially symmetric (3 - 9 min) and became polarized (12 min). In a *bud6*Δ cell (bottom), unseparated SPBs initiated movement toward the bud neck. As the SPBs separated (still far from the bud neck) Kar9p already favored one SPB (10 min). Kar9p continued to favor one pole as the spindle progressively aligned (15-30 min). Numbers indicate time elapsed in minutes. Bars, 2 μm.

SUPPLEMENTAL MATERIALS AND METHODS

Yeast strains and constructs

The alleles *bud6*Δ*, bni1*Δ*, bnr1*Δ (Delgehyr et al., 2008), *num1Δ* (Segal et al., 2000), *mad2*Δ (Huisman et al., 2007), *myo4Δ,* and *swe1Δ* were generated using KAN^R cassettes amplified by PCR (Wach et al., 1994). Deletions were confirmed by PCR analysis. Plasmid YIplac128 *bni1-FH2#1t* linearized with StuI was used to introduce the allele *bni1-FH2#1.* This plasmid contained a 2 kb BamHI - XhoI fragment of the 3' end of *BNI1* ORF that included the site of the mutations (Sagot et al., 2002) and a 3' UTR amplified by PCR using yeast genomic DNA from strain PY3744 *bnr1Δ bni1-FH2#1* (kindly provided by David Pellman, Dana-Farber Cancer Institute, Harvard Medical School). Strains a *MYO2:HIS3* and a *myo2-16:HIS3* were progeny of the homozygous diploid strains ABY551 and ABY553 (Schott et al., 1999), respectively. *myo2-17* and *myo2-18* alleles (Schott et al., 1999) were introduced into 15D background by transformation with the plasmid pRS305myo2-17 or pRS305myo2-18 (kindly provided by Felipe Santiago, Cornell University) and a 15D *MYO2:LEU2* strain was used as wild type control. Strains expressing Kar9p-GFP_3 at endogenous level were generated by transformation with pRM3226 ((Moore and Miller, 2007); a gift from Rita Miller, Oklahoma State University) linearized with ClaI. For GFP_3 tagging of endogenous Kar9p using *LEU2* as a selectable marker, YIplac128-KAR9t-GFP_3 linearized with StuI was used instead. This plasmid pCFP-TUB1 was used to express a CFP-Tub1p (Jensen et al., 2001). YIplac128-SPC42t-CFP or YIplac128-SPC42t-mCherry contained a 460 bp EcoRI - NotI fragment of the 3' end of the *SPC42* ORF generated by PCR fused in frame to CFP or mCherry, respectively. Linearization with NruI targeted integration at the endogenous *SPC42*. pRS404BFA1t-GFP contained a 750 bp SacI - NotI fragment of the *BFA1* 3' end of the ORF fused in frame to GFP. The construct was linearized with SphI for integration at the endogenous *BFA1*.

Cell cycle synchronization, time course and live imaging experiments

Time course experiments following release from G1 arrest were carried out as follows. Cells from a logarithmic culture grown in synthetic dextrose medium were collected and resuspended in YEPD containing 200 ng/ml alpha factor for 2 hours. After arrest was verified by microscopy, cells were rinsed and resuspended in synthetic medium to 8 x 10^6 cells/ml. Cell aliquots were taken every 15 minutes and fixed in 3.7% formaldehyde for 30 minutes to be used later for scoring budding index and progression of the spindle pathway. During the time course, cells were monitored live for bud emergence to ensure that actin depolymerization was induced after buds had formed. At the indicated time points for each experiment, the culture was split for paired treatments with 100µM Latrunculin B (LatB -prepared as 100x stocks in DMSO) or 10% DMSO (control). Aliquots were removed after 15 or 30 min and used immediately for acquiring fluorescence images of Kar9p-GFP_3 and CFP-Tub1p as five-Z stacks. 200µM LatA was used to disrupt actin cables and patches (Irazoqui et al., 2005). Aliquots of cells were fixed in 3.7% formaldehyde for 30 min and processed for rhodamine-phalloidin staining to verify the effectiveness of each treatment (not shown).

When indicated, cells were released from G1 arrest into synthetic medium containing 0.1 M hydroxyurea to increase the temporal window in which the cells contain short spindles to allow for comparison of "early" (during spindle assembly) or "late" (after the spindle is assembled and oriented) treatment with LatB prior to spindle elongation.

Time course experiments in synchronous populations subject to a temperature shift (*bnr1*Δ and *bnr1*Δ *bni1-FH2#1* strains) were carried out by incubating a logarithmic culture at 23°C in YEPD containing 200 ng/ml alpha factor. Cells were released in fresh synthetic dextrose medium at the same temperature and monitored live for bud emergence. At 45 min after release from G_1, cells were transferred to 34°C and samples were taken every 15 min for acquiring five-Z stacks of fluorescence images.

Nocodazole treatment was carried out by incubating 1 x 10^7 cells/ml in YEPD medium containing 1% DMSO and 15µg/ml nocodazole for 45 min (wild type and *mad2*Δ cells were also treated for 30 min). Cells were then rinsed and resuspended in fresh synthetic medium at a concentration of 1 x 10^7 cells/ml. Aliquots were harvested at 10-minute intervals and used immediately for acquiring fluorescence images of Kar9p-GFP3 and SPC42p-CFP or CFP-Tub1p later used for quantitation.

For time lapse recordings following nocodazole washout, cells were initially handled as for time course experiments. After nocodazole washout, following a 5 min incubation in synthetic dextrose medium, cells were concentrated by centrifugation and mounted on the same medium containing 25% gelatin. Recordings began ~ 15 min after nocodazole washout and were carried out by acquiring three-Z stacks of YFP/CFP images at 1, 3 or 5 min intervals. For time lapse recordings following LatB treatment, cells were first synchronized in G1 using 200 ng/ml alpha factor, released into fresh medium and treated with LatB as indicated for the time course experiments. Cells were washed and resuspended into fresh medium and immediately mounted to begin recordings.

Table S1. Yeast strains used in this study

Strain	Relevant Genotype
CYTK1	*MAT**a** bar1::LEU2 KAR9::KAR9:GFP$_3$(TRP1) ura3::HIS3:CFP:TUB1(URA3)*
CYTK2	*MAT**a** bar1::LEU2 bud6::KAN^R KAR9::KAR9:GFP$_3$(TRP1) ura3::HIS3:CFP:TUB1(URA3)*
CYTK3	*MAT**a** bar1::LEU2 bni1::KAN^R KAR9::KAR9:GFP$_3$(TRP1) ura3::HIS3:CFP:TUB1(URA3)*
CYTK4	*MAT**a** bar1::LEU2 bud6::KAN^R bni1::KAN^R KAR9::KAR9:GFP$_3$(TRP1) ura3::HIS3:CFP:TUB1(URA3)*
CYTK6	*MAT**a** bar1::LEU2 myo4::KAN^R KAR9::KAR9:GFP$_3$(TRP1)ura3::HIS3:CFP:TUB1(URA3)*
CYTK7	*MAT**a** bar1::LEU2 swe1::KAN^R KAR9::KAR9:GFP$_3$(TRP1) ura3::HIS3:CFP:TUB1(URA3)*
CYTK8	*MAT**a** bar1::LEU2 num1::KAN^R KAR9::KAR9:GFP$_3$(TRP1) ura3::HIS3:CFP:TUB1(URA3)*
CYTK9	*MAT**a** bar1Δ bnr1::KAN^R KAR9::KAR9:GFP$_3$(TRP1) ura3::HIS3:CFP:TUB1(URA3)*
CYTK10	*MAT**a** bar1Δ bnr1::KAN^R bni1::bni1-FH2#1(LEU2) KAR9::KAR9:GFP$_3$(TRP1) ura3::HIS3:CFP:TUB1(URA3)*
CYTK11	*MAT**a** bar1Δ MYO2:LEU2 KAR9::KAR9:GFP$_3$(TRP1) ura3::HIS3:CFP:TUB1(URA3)*
CYTK12	*MAT**a** bar1Δ myo2-17:LEU2 KAR9::KAR9:GFP$_3$(TRP1) ura3::HIS3:CFP:TUB1(URA3)*
CYTK13	*MAT**a** bar1Δ myo2-18:LEU2 KAR9::KAR9:GFP$_3$(TRP1) ura3::HIS3:CFP:TUB1(URA3)*
CYSK1	*MAT**a** bar1Δ KAR9::KAR9:GFP$_3$(TRP1) SPC42::SPC42:CFP(LEU2)*
CYSK2	*MAT**a** bar1Δ mad2::KAN^R KAR9::KAR9:GFP$_3$(TRP1) SPC42::SPC42:CFP(LEU2)*
CYSK3	*MAT**a** bar1Δ bud6::KAN^R KAR9::KAR9:GFP$_3$(TRP1) SPC42::SPC42:CFP(LEU2)*
CYSK5	*MAT**a** bar1Δ bni1::KAN^R KAR9::KAR9:GFP$_3$(TRP1) SPC42::SPC42:CFP(LEU2)*
CYSK6	*MAT**a** bar1Δ bni1::KAN^R bud6::KAN^R KAR9::KAR9:GFP$_3$(TRP1) SPC42::SPC42:CFP(LEU2)*
CYSK7	*MAT**a** bar1Δ KAR9::KAR9:GFP$_3$(TRP1) SPC42::SPC42:mCherry(LEU2)*
CYSK8	*MAT**a** bar1Δ bud6::KAN^R KAR9::KAR9:GFP$_3$(TRP1) SPC42::SPC42:mCherry(LEU2)*
CYTKM1	*MAT**a** MYO2:HIS3 his3 ura3 leu2 KAR9::KAR9:GFP$_3$(LEU2) ura3::HIS3:CFP:TUB1(URA3)*
CYTKM2	*MAT**a** myo2-16:HIS3 his3 ura3 leu2 KAR9::KAR9:GFP$_3$(LEU2) ura3::HIS3:CFP:TUB1(URA3)*
CYTKM3	*MAT**a** his3 ura3 leu2 KAR9::KAR9:GFP$_3$(LEU2) tub2C354S:URA3 trp1::HIS3:CFP:TUB1(TRP1)*

All strains were isogenic to 15DauA (a *ade1 his2 leu2-3,112 trp1-1a ura3Dns arg4*) except CYTKM1 and CYTKM2 that were derived from ABY551 and ABY553 (Schott et al., 1999)

SUPPLEMENTAL REFERENCES

Jensen, S., Segal, M., Clarke, D.J., and Reed, S.I. (2001). A novel role of the budding yeast separin Esp1 in anaphase spindle elongation: evidence that proper spindle association of Esp1 is regulated by Pds1. J. Cell Biol. *152*, 27-40.

Wach, A., Brachat, A., Pohlmann, R., and Philippsen, P. (1994). New heterologous modules for classical or PCR-based gene disruptions in Saccharomyces cerevisiae. Yeast *10*, 1793-1808.

Cepeda-García_Fig. S1

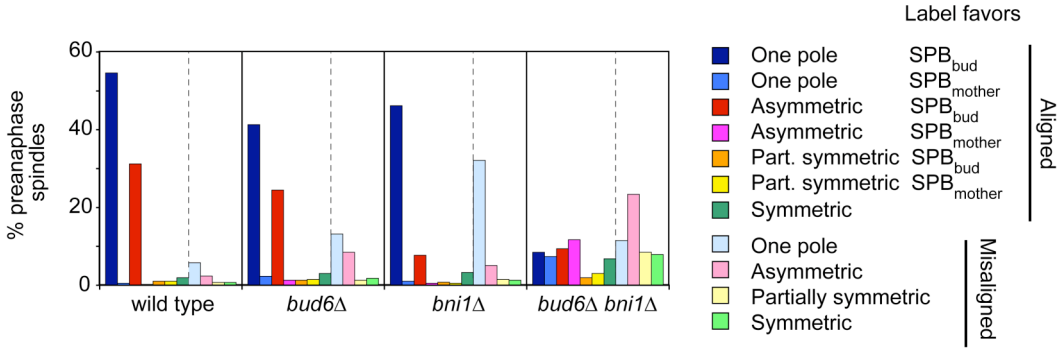

Cepeda-García_Fig. S2

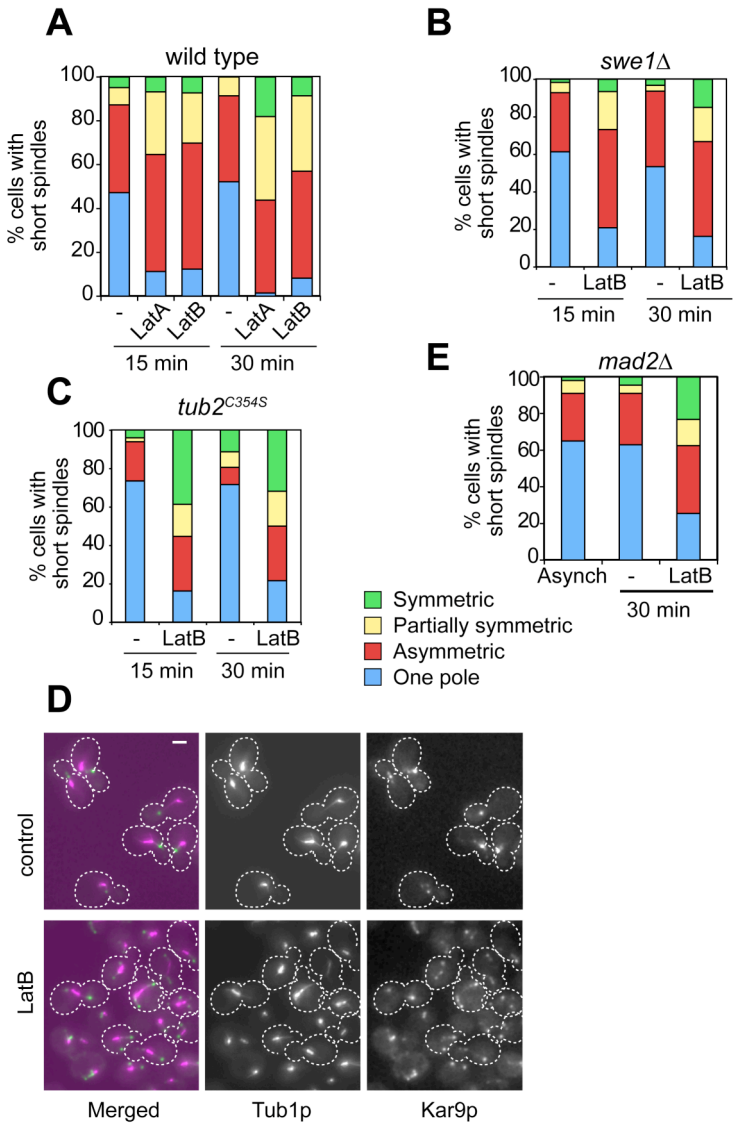

Cepeda-García_Fig. S3

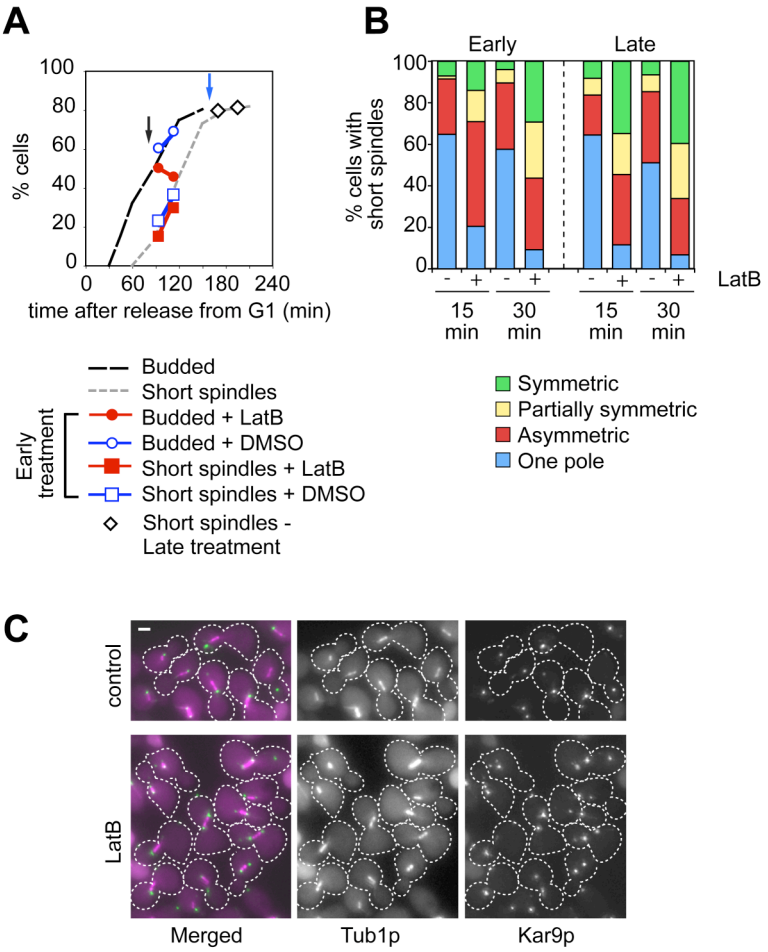

Cepeda-García_Fig. S4